

Identification of Buildings Damaged by Natural Hazards Using Very High-Resolution Satellite Images: The Case of Earthquake in L'Aquila, Italy



Luigi Barazzetti and Branka Cuca

Abstract Earth observation technologies are becoming increasingly important not only in monitoring practice in environmental domain, but also for detecting changes in urban areas caused by natural hazards such as earthquakes, floods or landslides. A range of high- and very high-resolution sensors useful for this purpose have been implemented as equipment of several missions launched since the year 2000, mostly by private companies. This chapter proposes a methodology for identification of damages in urban fabric of L'Aquila, caused by an earthquake in 2009. The images employed for assessment of such damages are Quickbird images with less than 1 m resolution, providing inputs for an advanced visualisation technique. The results of this process were discussed within a larger framework of emergency management cycle for possible thematic mapping, useful especially for response and recovery planning strategies.

Keywords L'Aquila · Earthquake · Quickbird · HR satellite imagery · Remote sensing · Historic centre

Introduction

A timely damage evaluation and risk assessment is becoming increasingly more important not only for humanitarian and social but also economic reasons and management purposes. Already in the 1990s, the benefits of the geographic information systems were explored for purposes of the comprehensive emergency management

L. Barazzetti (✉)

Department of Architecture, Built Environment and Construction Engineering (ABC),
Politecnico di Milano, Milan, Italy
e-mail: luigi.barazzetti@polimi.it

B. Cuca

Department of Civil Engineering and Geomatics, Faculty of Engineering and Technology,
Cyprus University of Technology, Limassol, Cyprus

© Springer Nature Switzerland AG 2020

D. G. Hadjimitsis et al. (eds.), *Remote Sensing for Archaeology and Cultural Landscapes*, Springer Remote Sensing/Photogrammetry,
https://doi.org/10.1007/978-3-030-10979-0_9

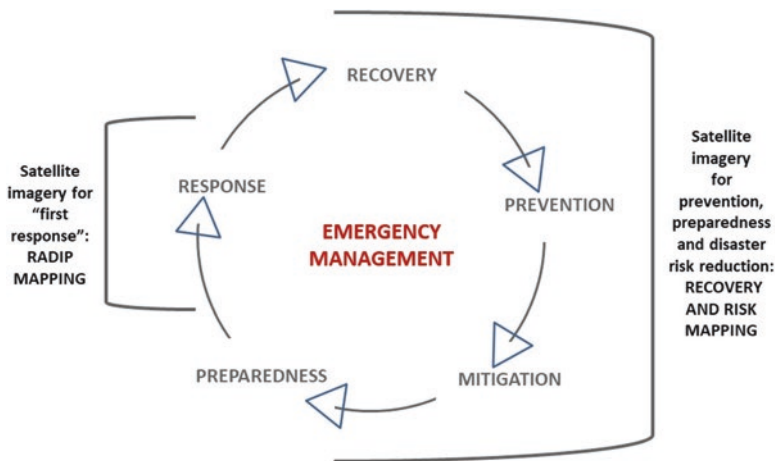


Fig. 1 Phases of emergency management cycle and types of services that can be provided by satellite remote sensing

(CEM) that relies on the temporal dimension of disasters to organise the emergency management process into a cycle of often overlapping phases (Cova 1999).

The European Copernicus Emergency Management Service (EMS) provides a set of mapping services using the satellite data provided by the Copernicus programme, to address the emergency situations resulting from natural or man-made disasters. In particular, mapping provided by EMS follows two temporal modes: rapid mapping to support emergency management activities immediately after a hazard has occurred and risk and recovery mapping in support of activities successive to immediate response, i.e. prevention, preparedness, risk reduction and recovery phases (Copernicus EMS 2018). According to this logic, Fig. 1 illustrates a schema proposal of services based on satellite earth observation (EO) technologies matching the phases of emergency management cycle.

Unlike fire or in some cases even flooding events (Alexakis et al. 2014), earthquakes cannot be prevented and cannot be controlled. For this reason, the focus of emergency management strategies in these cases is on phases of preparedness and response, i.e. on measures aimed at (i) reducing the risk, (ii) enhancing earthquake resistance, (iii) improving earthquake detection and monitoring and (iv) developing a response plan (Stovel 1998). In case of an earthquake in fact, the phase regarding damage evaluation is highly important for the first emergency response for securing of people, animals and structures and during the recovery phase in order to support assistance and inspection teams. Furthermore, such evaluations can be valuable also to reconsider the phases preceding the event (such as prevention, mitigation and preparedness) providing inputs to evaluation of economic damage and future urban planning and resilience strategies.

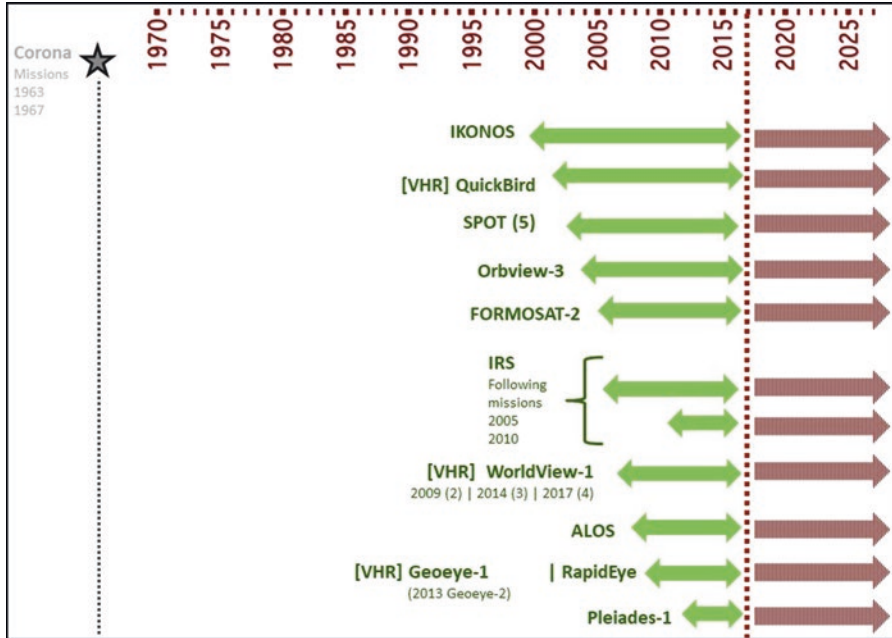


Fig. 2 Satellites with high- and very-high (indicated as VHR) resolution sensors for monitoring of urban environment: a timeline overview according to image availability

For cultural heritage and historic buildings, assessment and mapping of damage conducted by professionals become of extreme importance not only due to their cultural and social value, but also economic value for the community. Historic district and historic centres, for example, in addition to damages of buildings, can suffer also significant damages to their systems such as destruction of municipal infrastructure system (electrical and communication systems, water, gas and sewerage systems) and damage to transport infrastructures (including bridges, underpasses or elevated passages) potentially compromising the access to threatened or damaged areas (Stovel 1998). Timely and updated information is hence needed already in the first phases of emergency management in order to proceed with the quick and efficient response and recovery planning phases.

Damage assessment using satellite remote sensing has already been widely applied, especially cases of destruction occurring in urban areas (Rezaeian 2010; Pacifici et al. 2010; Dong and Shan 2013). The use of high- and very high-resolution images has proven to be valuable not only for visual inspection (Yamazaki et al. 2005) but also for pixel-based methods and classification focusing on the roofs of the buildings to access the damages (Chesnel et al. 2007). Fig. 2 illustrates selections of satellites with high- and very high-resolution sensors currently active, organised according to their year of launch. For a more exhaustive description on the civilian satellite systems, the reader is referred to Belward and Skøien (2015).



Fig. 3 Several scenes of L'Aquila historic centre, severely damaged during the earthquake occurred in 2009

Case Study: Town of L'Aquila in Italy

The case study examined by this chapter is the town of L'Aquila located in the central Italy, in Abruzzo Region. L'Aquila is erected on a soil with such a structure that amplifies seismic waves. In the past, the city was struck by earthquakes in 1315, 1349, 1452, 1501, 1646, 1703, 1706 and 1958 (Antonini 2010).

The earthquake that has struck L'Aquila on 6 April 2009 had an intensity of 5.8–5.9 on the Richter scale, and it has caused 309 human victims in the area. Quite a few buildings, especially in the historic centre that are still surrounded by the mediaeval walls, have undergone serious structural damages (Fig. 3).

As a consequence, almost complete evacuation of the historic centre has been imposed by the civil protection and is still in force for majority of the residential buildings. More than 65,000 inhabitants were forced to leave their homes. Many of the



Fig. 4 Perimeter of L'Aquila historic centre shown in white (a); damages of Santa Maria Paganica (b) and of L'Aquila Duomo cathedral (c), background images ©Google

buildings that have undergone damages were churches or other monuments of historic and cultural relevance to the citizens of L'Aquila and the whole region (Fig. 4).

The damages caused by the earthquake opened discussions about the anti-seismic building standards adopted in Italy. Although many buildings in L'Aquila have been built before the adoption of modern anti-seismic regulations, serious damages have been found also for recent buildings.

According to the Italian National Institute of Geophysics and Volcanology (INGV), in 2003 the whole territory of the country has been classified into four main categories in relation to the intensity and frequency of observed past events and according to application of specific normative construction measures in the seismic areas. These categories (sorted by decreasing risk intensity), are: Zone 1, area at major risk where strong earthquakes can occur; Zone 2, area where strong earthquakes can occur; Zone 3, area where earthquakes may occur but rarely; and Zone 4, less dangerous areas where earthquakes are rare.

An important fact is that, with this new classification conducted after the legislation measure has been introduced, the category "non-classified" has been cancelled and a new category Zone 4 has been introduced, thus bringing to consider the whole Italian territory as possibly subjected to the consequences of an earthquake. For Zone 4, it has been left up to single regional authorities to recommend measures for anti-seismic construction (for more details, reader is referred to Gazzetta Ufficiale n.105 2003). Regarding all categories, a base value of risk has been taken into account and defined considering a matrix of 5 km by 5 km, independently of administrative boundaries (Fig. 5c). Figure 5 shows illustration of seismic risk as provided by INGV, with reference to the values of the maximum acceleration of the soil. It can be noticed that the town of L'Aquila has been classified among the areas at the highest risk even before the tragic event occurred in 2009.

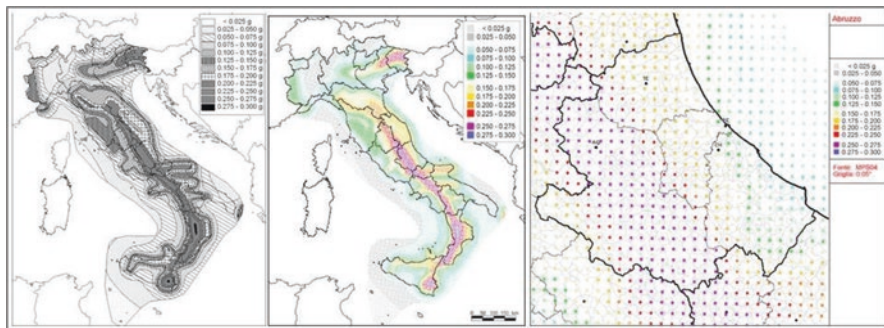


Fig. 5 Seismic risk reference in Italy: (left) the map in black and white, Official Gazette n.108; (middle) ag values on a 0.05° grid for the whole national territory; (right) ag values on a 0.05° grid, closeup on Abruzzo Region. (Source © INGV)

Dataset Description and Image Classification

The methodology proposed was focused on imagery collected above the historic centre of L'Aquila. The dataset is composed of two Quickbird images termed Ipre and Ipost provided by DigitalGlobe Inc., acquired on 4 September 2006 and 8 April 2009, respectively, with a ground resolution (GSD) of about 0.6 m. They also have a different off-nadir angle (10.65° and 5.6°), which is a significant issue for automated change detection. Indeed, the use of variable off-nadir angles allows reducing revisit time, but, in the case of tall objects, the top is leaning away from its base. In other words, there is a lack of overlap between objects, especially when large off-nadir angles are used.

The research work carried out concerns a procedure for comparing images with such additional spatial inconsistency, in which specific algorithms allow the user to handle geometrically inconsistent data. Here, the comparison of two images is not a pixel-to-pixel approach: objects in the images are extracted through object-based classification (Blaschke 2010) and are then compared after aligning classification shapefiles. The method assumes that residual misalignments are mainly caused by elongated features (not by areas indicating damage), which are then removed through object-based image analysis. The schema of the overall workflow is shown in the Fig. 6.

Preliminary data processing consists in pan-sharpening and orthorectification with the provided RPC coefficients. It is well known that VHR images suffer for the estimation of the true spatial orientation of every scan line for the direct measurement of sensor orientation. Orthorectification requires accurate grid models of the ground and 3D points with known coordinates to correct orientation biases. Quickbird has a geolocation accuracy of 23 m (CE90%), whereas panchromatic and multispectral images have a ground sampling distance (GSD) of 0.6/0.7 m and 2.4/2.5 m, respectively (DigitalGlobe 2013).

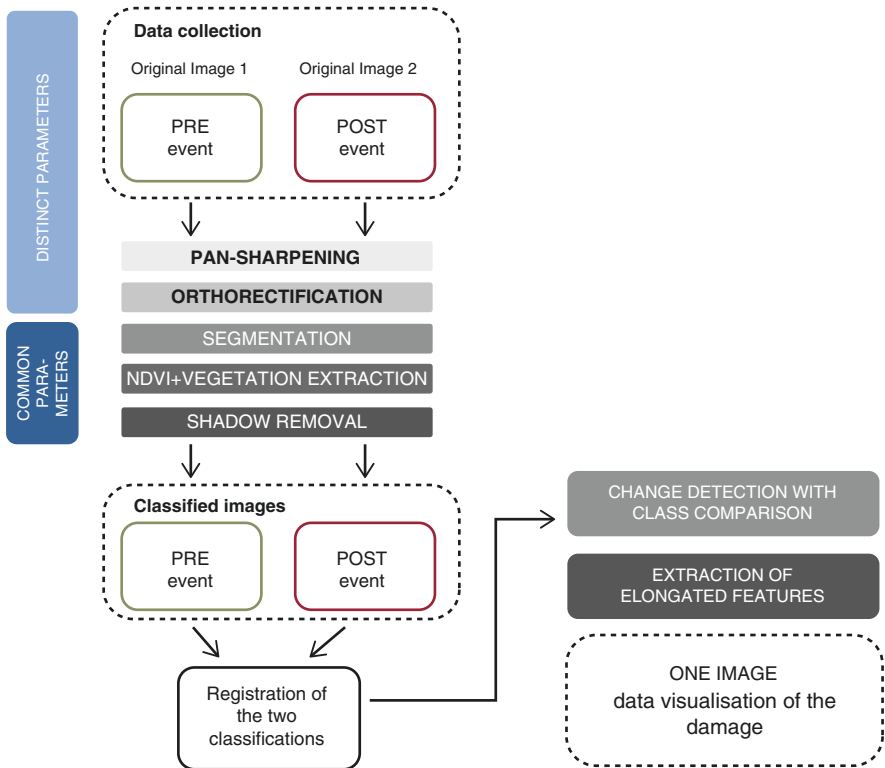


Fig. 6 The overall workflow for processing of single images and the couple (before/after the event)

Object-based image analysis can improve the classification accuracy of VHR satellite images. The proposed approach is based on three layers, which were assumed as sufficient for L’Aquila. Segmentation was carried out with the multi-resolution tool available in eCognition; areas with vegetation were then detected and excluded from data processing. The NDVI is computed for both images; then a threshold is used to classify objects as vegetation for both pre- and post-event images. Classification layers are termed V_{pre} and V_{post} .

The second class used is related to shadows, which are classified using brightness $BRI = [R + G + B]/3$. This has provided two new classes (S_{pre} , S_{post}). Finally, a class “object” is assigned to pixel which does not belong to the previous classes, obtaining two new layers termed O_{pre} and O_{post} . Results for a selected area close to the Spanish Fortress in L’Aquila (district of the church Santa Maria Paganica) are shown in Fig. 7. As it can be seen, the class object does not discriminate between buildings and roads that appear in the same class (Fig. 7b, in red colour).

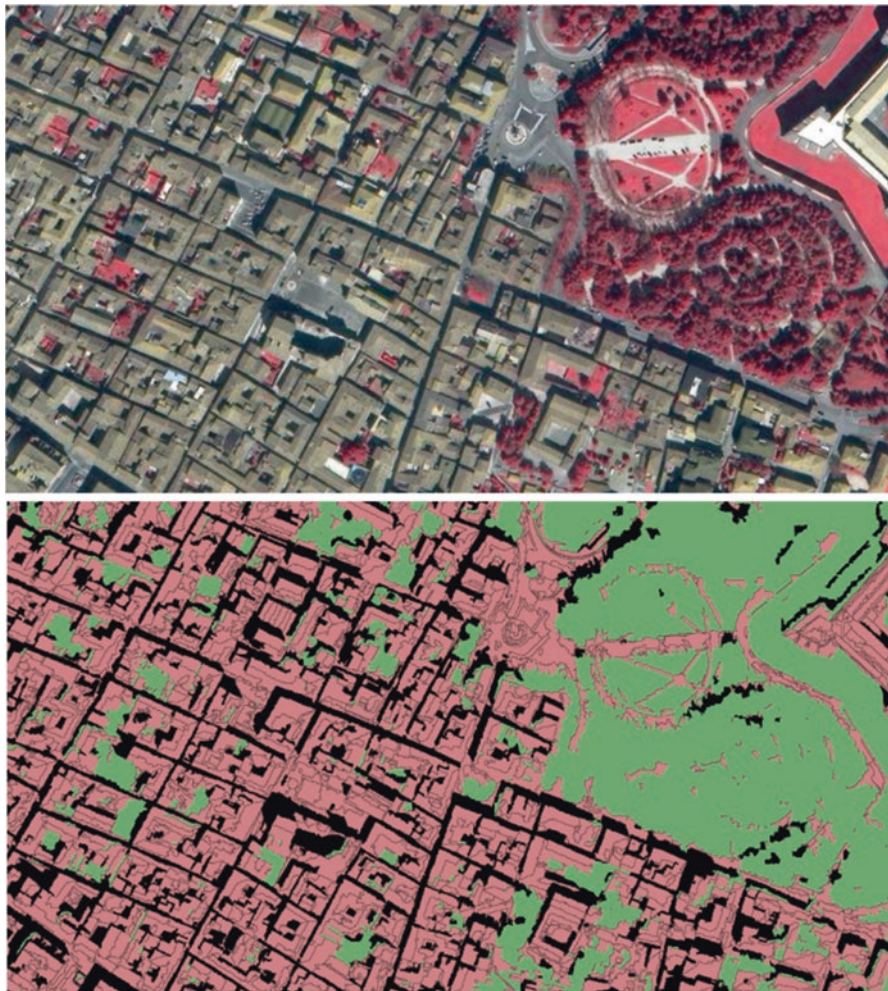


Fig. 7 The Quickbird image after the earthquake and classification results of segmented elements

Change Detection with Variable Off-Nadir Angle

Change detection requires the vector layers generated in the previous object-based classification. The method does not consider those buildings that have completely collapsed during the earthquake. The main assumption is that if the shadow of a building is found only in the post-event image, that shadow indicates a local damage like the collapse of the roof. The idea is to identify only those areas of shadow found in the post-event satellite image; hence the proposed procedure allows the identification of partially damaged buildings.

Change detection with images acquired with a different off-nadir angle does not allow a direct pixel-to-pixel comparison. After preliminary data processing, images exhibit a significant lack of pixel also caused by the digital elevation model (DEM) and the rational polynomial coefficients (RPC) without bias compensation (Hanley et al. 2002; Fraser and Hanley 2003). On the other hand, quick data processing after the earthquake can be guaranteed only if the analysis is based on the available products, without a mission on-site in order to avoid that operators are exposed to any possible risks. For instance, correcting the bias in the RPC coefficients would require some ground control points measured with GNSS receivers. This practice is not always feasible, especially in areas with a potential risk for the safety of human operators, such as in case of earthquakes and areas that might be subject to so-called aftershocks.

In order to overcome this problem, an additional registration procedure was developed to reduce the geometric discrepancy between the classification shapefiles. The final result is not a perfect correspondence between different vector layers. However, a strong reduction of the initial misalignment can be achieved. For these procedures, images are divided into tiles, and matching is carried out to detect corresponding points between the images. Then, an additional check has been added to remove wrong image correspondences through robust estimation of homographic transformations. The threshold between inliers and outliers is set to geolocalisation accuracy of Quickbird data (CE90%). The use of small tiles (instead of the full image) allows one to locally reduce deformities, and the estimation of the homography is more consistent with the global error due to RPC coefficients without bias compensation. The computer parameters are then applied to the classification.

Before running the change detection algorithm (comparison of classification layers), the intersection between the shadow layers after the earthquake S_{post} and both vegetation V_{pre} and shadows S_{pre} before the earthquake is carried out, and the identified areas are excluded from data processing. This can be written as $S_{post} \cap (V_{pre} \cup S_{pre})$. Then, the intersection written as $(S_{post} \setminus S_{post} \cap (V_{pre} \cup S_{pre})) \cap O_{pre}$ is computed to find partial damages. This second intersection is affected by the variable off-nadir angle, which has caused an additional generation of elongated elements in areas close to the polygon edges of classification shapefiles. Removing such elements from the analysis is mandatory to improve change detection results and hence to identify only those areas that depict shadows of buildings in post-event image.

As such errors have an elongated shape, geometric parameters based on their geometry can separate them from effective damages, which have a more circular form. Given a generic element E_i , the index $T_i = \sqrt{P_i} / \left(\sqrt{\sigma_{x_i}^2 + \sigma_{y_i}^2} + 1 \right)$ has low value for elongated feature and large values for squared objects. $\sqrt{P_i}$ is the diameter of a square object made up of P_i pixels, and $\sigma_{x_i}^2$ and $\sigma_{y_i}^2$ are the variances. The interactive manual setting of the threshold $[T_{min}, T_{max}]$ allows one to find the proper parameters for extracting only local damages.



Fig. 8 The area around the church of Santa Maria Paganica: (a, c) Pre- and (b, d) post-event images. The comparison of classification shapefiles provide several errors shown in red colour (e), which are automatically filtered out with the removal of elongated features showing only shadows that indicated the damage, shown in yellow colour (f)

An example of a damaged building examined by this method is the church of Santa Maria Paganica. Figure 8 shows the building and the neighbourhood area before (a, c) and after (b, d) the earthquake. The comparison of classification shapefiles provides several errors (e), which are automatically filtered out with the removal of elongated features, showing only those shadows that with the highest probability indicate the damage caused by the earthquake (f).

Discussion of Work

The proposed solution is based on different steps, in which several parameters have to be set, firstly considering the two images separately and then as a couple. The whole workflow can be easily automated as it is made up of consequential steps. Most operations do not require a significant computation cost, apart from the multiresolution

segmentation which could become quite slow for big images. The method proposed is to be considered as an advanced visualisation technique rather than a method to compute the number of damaged buildings. Hence, the threshold can be interactively modified by the user to enhance the visualisation of the damaged building. Indeed, it is not simple to define a priori all the thresholds in the different steps of the workflow, especially in case of replication of the methodology in other areas. At the moment, the method has been tuned for the specific case for the town of L'Aquila.

The logic behind the whole procedure is similar to the grading maps provided by Copernicus EMS rapid mapping products. For example, in the case of another disastrous earthquake event which occurred in Amatrice (Italy) in 2016, the service has provided “grading maps” – thematic maps derived from post-event images that provide an assessment of the damage grade. Such maps include the extent, magnitude or damage grades specific to each disaster type. In case of earthquakes, the grading map can be shown taking into account the number of destroyed damaged buildings in each cell of a regular grid.

In fact, the method proposed has also a strong connection with the logic of the geographic information systems (GIS) and spatial data infrastructures (SDI) in general. It provides vector shapefile layers as output, which can be further inspected and handled in GIS software, also in combination with other types of geospatial open data such as roads or other infrastructures for accessibility and danger verification. For example, an integration with the open-source QGIS platform can be performed (Fig. 9). The results can be further manipulated in an GIS software to enhance the visibility of damaged buildings.

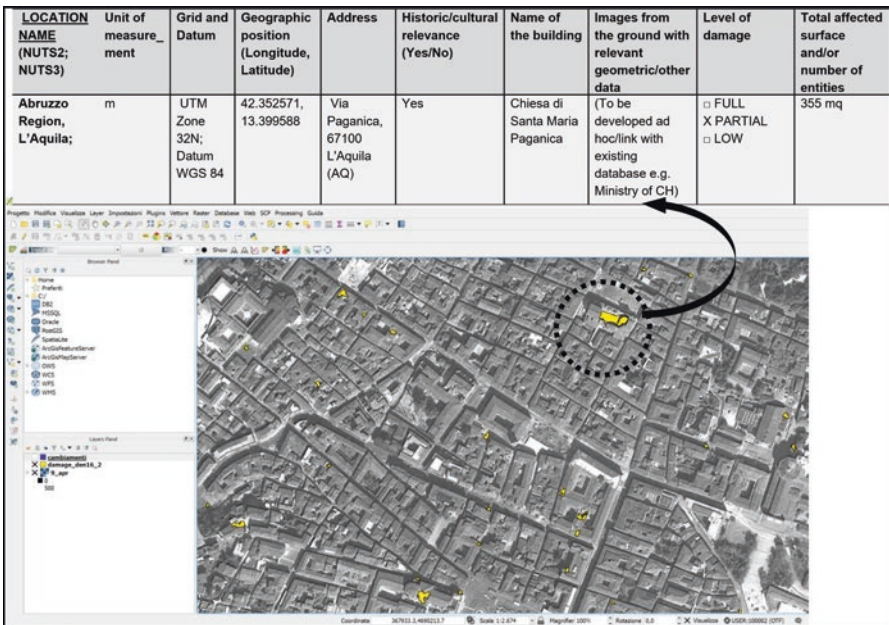


Fig. 9 The results of change detection with variable off-nadir angle very high-resolution imagery can be exported, manipulated and visualised in GIS software: L'Aquila case study

Figure 9 (below) shows the case in which only the feature with an elongation in a predefined range using the attribute table associated to the shapefile. As explained, the results here illustrated do not take into account fully destroyed buildings but rather those which have undergone partial damage. The table of Fig. 9 linked to the polygon of the undergone damage contains important information about the building itself such as geographic position (cartographic coordinates), projection and datum of the map, building address, name of the building (if any), historic/cultural relevance as “yes/no” (information provided by the regional public authority geoportal), images of the building from the ground with relevant geometric/other data (to be developed “ad hoc”), level of damage of the building (qualitative assessment in terms of low/partial/high level of damage) and total affected surface and/or number of entities damaged.

Conclusion

Since 2016 an official document issued by MiBACT (Italian Ministry of Cultural Heritage and Activities and of Tourism) has put into place a “Procedure of the Implementing Officer of 21 September 2016: management of activities on the securing of movable and immovable cultural heritage” (ordinanza n. 393 del 13 settembre 2016), nominating a body “Funzione Beni Culturali” as a responsible party with a one member of MiBACT and one member of civil protection as main representatives. Such initiative declares a great public commitment, and attention is currently on heritage affected by extreme earthquake events and sets the ground for a larger framework of intervention on built cultural heritage in a period of postcrisis such as in the case of L’Aquila here presented. This chapter illustrates how a methodology relying in photogrammetric and visualisation investigation techniques applied on high- and very high-resolution EO satellite data can contribute to the mapping of the damaged buildings in case of earthquake, providing both qualitative and quantitative information of a specific building, district or even entire complex (e.g. a historic centre of the city). The method could hence support the action of identification and quantification of such buildings and affected areas, both for processing of grading maps (in case of rapid mapping) and thematic mapping for risk and recovery purposes at the later stages of emergency management cycle.

Acknowledgement The authors would like to thank the DigitalGlobe Foundation (www.digitalglobefoundation.org) for providing the Quickbird images used in this work.

References

- Alexakis DD, Gryllakis E, Koutroulis A, Agapiou A, Themistocleous K, Tsanis I, Michaelides S, Pashiardis S, Demetriou C, Aristeidou K, Retalis A, Tymvios F, Hadjimitsis DG (2014) GIS and Remote Sensing Techniques for the Assessment of Land Use Changes Impact on Flood

- Hydrology: the Case Study of Yialias Basin in Cyprus, *Natural Hazards and Earth System Sciences* 14:413–426
- Antonini O (2010) *I terremoti aquilani*, Tau Editrice, 48 pages
- Belward AS, Skøien JO (2015) Who launched what, when and why; trends in global land-cover observation capacity from civilian earth observation satellites. *ISPRS J Photogramm Remote Sens* 103:115–128
- Blaschke T (2010) Object based image analysis for remote sensing. *ISPRS J Photogramm Remote Sens* 65:2–16
- “Copernicus Emergency Management Service.” Directorate Space, Security and Migration, European Commission Joint Research Centre (EC JRC). Accessed 2 Aug 2018. <http://emergency.copernicus.eu/>
- Cova TJ (1999) GIS in emergency management. *Geogra Inf Syst* 2:845–858
- Chesnel AL, Binet R, Wald L (2007) Quantitative assessment of building damage in urban area using very high resolution images. In: 2007 urban remote sensing joint event. IEEE, pp 1–5
- DigitalGlobe (2013) Geolocation accuracy of worldview products
- Dong L, Shan J (2013) A comprehensive review of earthquake-induced building damage detection with remote sensing techniques. *ISPRS J Photogramm Remote Sens* 84:85–99
- Fraser CS, Hanley HB (2003) Bias compensation in rational functions for Ikonos satellite imagery. *Photogramm Eng Remote Sens* 69(1):53–57
- Gazzetta Ufficiale n. 105, 8 May 2003, Supplemento Ordinario n. 72, Ordinanza del Presidente del Consiglio dei Ministri n.3274, March 20th, 2003 “Primi elementi in materia di criteri generali per la classificazione sismica del territorio nazionale e di normative tecniche per le costruzioni in zona sismica”
- Hanley HB, Yamakawa T, Fraser CS (2002) Sensor orientation for high-resolution satellite imagery. *Int Arch Photogramm Remote Sens* 34(1):69–75. (on CD-ROM)
- Pacifici F, Chini M, Bignami C, Stramondo S, Emery WJ (2010) Automatic damage detection using pulse-coupled neural networks for the 2009 Italian earthquake,” *International Geoscience and Remote Sensing Symposium 2010*, Honolulu, USA, July 25–30
- Rezaeian M (2010) Assessment of earthquake damages by image-based techniques, Diss.. ETH Zurich N. 19178, 149 pages
- Stovel H (1998) *Risk preparedness: A management manual for World Cultural Heritage*, Rome: ICCROM, 153 pages
- Yamazaki F, Yano Y, Matsuoka M (2005) Damage detection in earthquake disasters using high-resolution satellite images. *ICOSSAR 2005*:1693–1700